arXiv:cond-mat/0510294v1 [cond-mat.str-el] 11 Oct 2005

Exchange interaction in quantum rings and wires in the Wigner-crystal limit

Michael M. Fogler and Eugene Pivovarov
Department of Physics, University of California San Diego, La Jolla, California 92093
(Dated: March 23, 2022)

We present a controlled method for computing the exchange coupling in correlated one-dimensional electron systems based on the relation between the exchange constant and the pair-correlation function of spinless electrons. This relation is valid in several independent asymptotic regimes, including low electron density case, under the general condition of a strong spin-charge separation. Explicit formulas for the exchange constant are obtained for thin quantum rings and wires with realistic Coulomb interactions by calculating the pair-correlation function via a many-body instanton approach. A remarkably smooth interpolation between high and low electron density results is shown to be possible. These results are applicable to the case of one-dimensional wires of intermediate width as well. Our method can be easily generalized to other interaction laws, such as the inverse distance squared one of the Calogero-Sutherland-Moser model. We demonstrate excellent agreement with the known exact results for the latter model and show that they are relevant for a realistic experimental setup in which the bare Coulomb interaction is screened by an edge of a two-dimensional electron gas.

PACS numbers: 71.10.Pm, 73.21.Hb, 73.22.-f

I. INTRODUCTION

Much interest has been devoted to the spin degree of freedom in novel one-dimensional (1D) conductors, both of linear shape (carbon nanotubes,[1] semiconductor nanowires,[2] conducting molecules[3]) and recently, of a circular one (quantum rings[4,5,6]). Parameters of these systems, e.g., average distance between the electrons a, their total number N, their effective mass m, dielectric constant ϵ, effective Bohr radius $a_B = \hbar^2\epsilon/me^2$, *etc.*, can vary over a broad range or can be tuned experimentally. This creates an intriguing opportunity of reaching the Wigner-crystal (WC) limit,[7,8] $r_s \equiv a/2a_B \gg 1$, where electrons arrange themselves into a nearly regular lattice. According to numerical simulations,[8] the 1D WC is well formed already at $r_s > 4$. The corresponding electron densities are easily achievable but the presence of disorder has so far hindered experimental investigations of the 1D WC regime.[9] Remarkably, the unwanted disorder can apparently be substantially suppressed in the case of carbon nanotubes *suspended* above a substrate. In such devices very large r_s with no immediately obvious disorder effects have been recently demonstrated.[10] Due to a finite length of the nanotubes used, they contained only a few electrons (< 30) in the $r_s > 4$ regime. (Such systems are commonly referred to as Wigner molecules.) These encouraging progress on the experimental side and a recent revival of interest to the 1D WC on the theoretical side[11] have motivated us to undertake in the present paper a careful investigation of the fundamental energy scales that govern the spin dynamics in 1D Wigner crystals and molecules.

In a strict academic sense, the term "crystal" should not be used in 1D because the phonon-like vibrations of the putative lattice are infrared divergent. It is nevertheless true that at $r_s \gg 1$ the pair correlation function

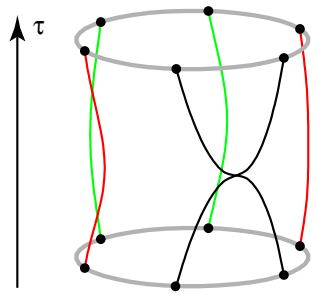


FIG. 1: (Color online) A sketch of the instanton trajectories for the six-electron Wigner molecule on a ring.

(PCF)

$$g(x) = \frac{1}{Nn}\sum_{i\neq j}\langle\delta(x_i - x_j - x)\rangle \qquad (1)$$

is sharply peaked at integer multiples of a. Here x_j are electron coordinates. Thus, for the study of electron correlations in Wigner molecules or in a group of few nearby electrons in an infinite wire the WC concept is fully adequate. Once adopted, this concept implies[12] that the low-energy dynamics of electron spins is dominated by the nearest-neighbor Heisenberg interaction of strength J proportional to an exponentially small probability of quantum tunneling under the Coulomb barriers that separate the adjacent electrons. Exchanges of more distant neighbors are penalized with a much stronger tunneling suppression and can therefore be neglected.

As a result of the exponential smallness of the exchange coupling J, the energy scales for orbital and spin dynamics are drastically different. This *strong* spin-charge separation is expected to cause anomalies in many essential electron properties, e.g., ballistic conductance[11] of quantum wires and persistent current of quantum rings.[13] To

systematically explore such phenomena a reliable estimate of the exchange coupling J is needed. This has been an important open problem however. The smallness of J makes it difficult to compute even by rather advanced computer simulations.[13] Attempts to derive J analytically (for the nontrivial case $N > 2$) have so far been based on the approximation that neglects all degrees of freedom in the problem except the distance between the two interchanging electrons.[11,14] We call this a Frozen Lattice Approximation (FLA). The accuracy of the FLA is unclear because it is not justified by any small parameter. When a given pair does its exchange, it sets all other electrons in motion, too (Fig. 1). Simple dimensional considerations (confirmed by the calculations below) show that the maximum tunneling displacements of the electrons nearby the first pair reach a fraction of a, i.e., they are at most numerically, but not *parametrically*, small. In view of the aforementioned and other recent experimental[15,16] and theoretical[17,18,19] work on spin-related effects in 1D conductors a controlled calculation of J seems a timely goal. It is accomplished in this paper, where we treat the spin exchange in a Wigner molecule (or a WC) as a true many-body process and compute J to the leading order in the large parameter r_s. A brief account of this work has been reported in Ref. 20. The same problem has been independently studied by Klironomos *et al.*[21] and wherever they can be compared our results agree.

The paper is organized as follows. The definition of the model and our main results are given in Sec. II. The step-by-step derivation for the simplest nontrivial case of a three-electron molecule is presented in Sec. III. The $N > 3$ case is discussed in Secs. IV and V. An alternative route to the derivation of J is outlined in Sec. VI. The comparison with the known analytical results for related models is done in Sec. VII. The issues relevant to the current experiments are addressed at the end of Sec. VII and in Sec. VIII. The concluding remarks are in Sec. IX.

II. MODEL AND MAIN RESULTS

We assume that electrons are tightly confined in the transverse dimensions on a characteristic lengthscale ("radius" of the wire) $R \ll a_B$. In this case the energy separation $\hbar^2/mR^2$ of the 1D subbands greatly exceeds the characteristic Coulomb interaction energy $e^2/\epsilon R$. Assuming that only the lowest subband is occupied, the Hamiltonian can be projected onto the Hilbert space of this subband. This turns the problem into a strictly 1D one, with the Coulomb law replaced by an effective interaction $U(r)$ that tends to a finite value at distances $r \ll R$. The precise form of U depends on the details of the confinement. For simplicity, we adopt a model[22,23]

$$U(r) = \frac{e^2}{\epsilon}\frac{1}{r+R}, \tag{2}$$

N	3	4	6	8	∞	∞-FLA
η	2.8009	2.7988(2)	2.7979(2)	2.7978(2)	2.7978(2)	2.8168
κ	3.0448	3.18(6)	3.26(6)	3.32(7)	3.36(7)	2.20

TABLE I: Results for Wigner molecules on a ring (finite N) and for wires ($N = \infty$).

which nevertheless correctly captures both short- and long-range behavior of the interaction for *any* realistic confinement scheme and is similar to other expressions used in the literature,[24,25] see more in Sec. VIII. Most of our calculations below pertain to the ring geometry where r stands for the chord distance, $r = (Na/\pi)\,|\sin(\pi x/Na)|$, x being the coordinate along the circumference. At large r_s the electrons assume a Wigner-molecule configuration where they reside at the corners of a regular polygon. The effective low-energy Hamiltonian of such a state is given by

$$H = \frac{\hbar^2}{2I}L^2 + J\sum_j \mathbf{S}_j\mathbf{S}_{j+1} + \sum_\alpha n_a\hbar\omega_\alpha, \tag{3}$$

where L is the center-of-mass angular momentum, $\mathbf{S}_j$ are electron spins, and n_α are the occupation numbers of "molecular vibrations." (The same Hamiltonian applies to small-N quantum dots.[13]) At large r_s, the total moment of inertia I and the vibrational frequencies ω_α are easy to compute because they are close to their classical values. Our task is to calculate J, which is more difficult.

We show that the asymptotically exact relation exists between J and the PCF $g_0(x)$ of a *spin polarized* 1D system. For an ultrathin wire, $\mathcal{L} \equiv \ln(a_B/R) \gg 1$, it is particularly simple:

$$J = \frac{e^2a_B^2}{2\mathcal{L}\epsilon}g_0''(0), \quad r_s \gg \frac{1}{\mathcal{L}}. \tag{4}$$

By virtue of Eq. (4), the calculation of J reduces to an easier task of computing $g_0(x)$. For large r_s our final result has the form

$$J = \frac{\kappa}{(2r_s)^{5/4}}\frac{\pi}{\mathcal{L}}\frac{e^2}{\epsilon a_B}\exp\left(-\eta\sqrt{2r_s}\right), \quad r_s \gg 1, \tag{5}$$

where the values of η and κ are given in Table I together with the prediction of the FLA,[11,14] for comparison. [Klironomos *et al.*[21] independently obtained $\eta = 2.79805(5)$ for the case of a wire.]

In the remainder of the paper we give the derivation of the above results and discuss their consequences for various experimental and theoretical questions.

III. THREE-ELECTRON QUANTUM RING

We start with the simplest nontrivial example: three electrons on a ring. Let $0 \le x_j < 3a$, $j = 0, 1, 2$ be their

coordinates along the circumference. We will compute the exchange coupling J between the $j=0$ and the $j=1$ electrons. In the FLA the third electron remains at rest while the other two interchange, as in a classical picture. However, we will show that the consistent calculation of J requires taking quantum fluctuations of this third electron into account.

The system has the total of three degrees of freedom: the center of mass $x_{\rm cm}$, the distance between the exchanging electrons $x \equiv x_1 - x_0$, and the distance between the third electron and the center of mass, $X_2 \equiv x_2 - x_{\rm cm} - a$. We can restrict the variables x and X_2 to the fundamental domain, $|x| < 3a/2$, $|X_2| < a/2$, where only the chosen two electrons can closely approach each other. This allows us to ignore exchanges involving the $j=2$ electron, and hence, its spin. Ignoring also the irrelevant center-of-mass motion, we obtain the Hamiltonian

$$H_3 = -\frac{\hbar^2}{2\mu}\partial_x^2 - \frac{\hbar^2}{2M}\partial_{X_2}^2 + U_{\rm tot}(x, X_2), \tag{6}$$

where $\mu = m/2$ and $M = 3\mu$. The potential term

$$\begin{aligned} U_{\rm tot} &= U(x) + U_{\rm ext}, \\ U_{\rm ext} &= U\left[(3/2)(X_2+a) - x/2\right] \\ &\quad + U\left[(3/2)(X_2+a) + x/2\right], \end{aligned} \tag{7}$$

has two minima in the fundamental domain, at $x = \pm a$, $X_2 = 0$. The minima are separated by a high potential barrier at $x = 0$. They give rise to the two lowest-energy states of the system: the spin-singlet ground state, $\mathbf{S}_0 + \mathbf{S}_1 = 0$, with an orbital wavefunction $\Phi_s = \Phi_s(x, X_2)$ and a triplet with a wavefunction Φ_t. Their energy splitting is the desired exchange coupling J. In close analogy with Herring's classic treatment of H_2-molecule[26] (see also Ref. 27) for our $N=3$ "molecule" we obtain

$$J = \frac{2\hbar^2}{\mu}\int dX_2\ \Phi_1 \partial_x \Phi_1|_{x=0}\,, \tag{8}$$

where the (normalized to unity) "single-well" wavefunction $\Phi_1(x, X_2)$ is the ground-state of H_3 with a modified potential $U_{\rm tot} \to U_1 \equiv U_{\rm tot}(\max\{x, 0\}, X_2)$. Equation (8) is valid[26] to order $O(J^2)$; with the same accuracy,

$$\Phi_{s,t} = \frac{1}{\sqrt{2}}[\Phi_1(x, X_2) \pm \Phi_1(-x, X_2)]. \tag{9}$$

Let us discuss the form of the single-well wavefunction $\Phi_1(x, X_2)$. Near its maximum at $x = a$, $X_2 = 0$, it is a simple Gaussian,

$$\Phi_1(x, X_2) \propto \exp\left[-\frac{(x-a)^2}{2l^2} - \frac{M}{2\hbar}\omega(a) X_2^2\right], \tag{10}$$

where $l = [\hbar^2/\mu U''_{\rm tot}(a)]^{1/4} \sim r_s^{-1/4} a$ is the amplitude of the zero-point motion in x ($U_{\rm tot}$ written with a single argument is meant to be evaluated at $X_2 = 0$). The quantity

$$\omega(x) = \left[M^{-1}\partial_{X_2}^2 U_{\rm tot}(x)\right]^{1/2} \tag{11}$$

is real and positive in the classically forbidden region $0 < x < a - l$. Therefore, the tunneling barrier is the lowest and Φ_1 is the largest along the line $X_2 = 0$. Furthermore, it is easy to see that $\Phi_1(x, X_2)$ rapidly decays at $|X_2| \gtrsim l$. Since $l \ll a$, the following Gaussian approximation is justified in the *entire* fundamental domain of x:

$$\Phi_1 = \phi(x) \exp\left[-\frac{M}{2\hbar}\Omega(x) X_2^2\right]. \tag{12}$$

Acting on this *ansatz* with H_3 and neglecting the subleading terms $O(l/a)$, we obtain the following equations on $\Omega(x)$ and $\phi(x)$:

$$\partial_x \Omega = \frac{\Omega^2(x) - \omega^2(x)}{[(2/\mu)\Delta U_{\rm tot}(x)]^{1/2}}, \tag{13a}$$

$$\left\{\frac{\hbar^2}{2\mu}\partial_x^2 - U_{\rm tot}(x) - \frac{1}{2}\hbar\Omega(x) + E\right\}\phi(x) = 0, \tag{13b}$$

where $\Delta U_{\rm tot}(x) \equiv U_{\rm tot}(x) - U_{\rm tot}(a)$. We wish to comment that the basic idea of the Gaussian ansatz has been used previously for computing exchange constants in ^{3}He crystals,[28] but the simple closed form of Eqs. (13) has not been demonstrated.

Comparing Eqs. (10) and (12) we see that near $x = a$ function $\phi(x)$ takes the form,

$$\phi(x) = \left[\frac{M\Omega(a)}{\pi^{3/2}\hbar l}\right]^{1/2} e^{-(x-a)^2/2l^2}, \tag{14}$$

while $\Omega(x)$ satisfies the boundary condition $\Omega(a) = \omega(a)$. Resolving the 0/0 ambiguity in Eq. (13a) by L'Hôpital's rule we furthermore obtain

$$\Omega'(a) = \frac{\omega'(a)}{1 + \left\{\left(\frac{M}{16\mu}\right)\left[1 + U''(a)/U''_{\rm ext}(a)\right]\right\}^{1/2}}. \tag{15}$$

Finally, using this formula and straightforward algebraic manipulations one can fix the constant term E in Eq. (13b) to be

$$E = U_{\rm tot}(a) + \frac{\hbar}{2}\left[\omega(a) + \omega_0\right], \quad \omega_0 \equiv \frac{\hbar}{\mu l^2}. \tag{16}$$

Next consider the interior of the classically forbidden region, $x \ll a$. Since the tunneling barrier $\Delta U_{\rm tot}(x)$ is large here, Ω is a slow function of x. Taking advantage of the following expression for the PCF of a spin-polarized molecule,

$$g_0(x) \equiv 2\int \prod_{j=2}^{N-1} dX_j \Phi_t^2(x, X_2, \ldots, X_{N-1}), \quad |x| < \frac{3a}{2}, \tag{17}$$

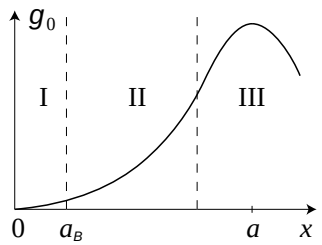


FIG. 2: The PCF of a spin-polarized system (schematically). Regions I, II, and III are described in the main text.

we find that Eq. (8) entails the relation

$$J = \frac{\hbar^2}{4\mu}\frac{\phi(0)}{\phi'(0)} g_0''(0). \tag{18}$$

Anticipating the discussion in Sec. IV, Eq. (17) is written for an arbitrary $N > 2$, with the notation $X_j \equiv x_j - x_{\rm cm} + (N-1-2j)(a/2)$ being used; the PCF is normalized as appropriate in the WC limit,

$$\int_0^{3a/2} g_0(x)dx = 1. \tag{19}$$

The dependence of g_0 on x that results from this formalism is sketched in Fig. 2. Near the $x = a$ maximum (region III), $g_0(x)$ is given by [cf. Eq. (10)]

$$g_0(x) = \left(1/\sqrt{\pi}\, l\right) \exp\left[-(x-a)^2/l^2\right]. \tag{20}$$

In the region II the quasiclassical approximation applies. In particular, at $a_B \ll x \ll a$ the result for $g_0(x)$ can be written in terms of the tunneling action,

$$S_3(x) = \frac{1}{\hbar}\int_x^a dy \left[2\mu \Delta U_{\rm tot}(y)\right]^{1/2}, \tag{21}$$

and the appropriate prefactor, as follows:

$$g_0(x) = \frac{a}{l^2}\left[\frac{1}{2\pi}\frac{\Omega(a)}{\Omega(x)}\frac{\hbar\omega_0}{U(x)}\right]^{1/2} e^{\xi(x)-2S_3(x)}, \tag{22}$$

$$\xi(x) = \int_x^a dy \left\{\frac{\omega_0 + \Omega(a) - \Omega(y)}{\left[(2/\mu)\Delta U_{\rm tot}(y)\right]^{1/2}} - \frac{1}{a-y}\right\}. \tag{23}$$

In comparison, the FLA[11] amounts to replacing $\Omega(x)$ by a constant in the above equations, thereby effectively ignoring the quantum fluctuations of the dynamical variable X_2. Finally, in an ultrathin wire, $\mathcal{L} \gg 1$, there is also region I, $x \lesssim a_B$, where the quasiclassical approximation breaks down. Fortunately, at such x, Eq. (13b) can be simplified, as $\Omega(x) \simeq \Omega(0)$ and $U_{\rm tot}(x) \simeq U(x) + 2U(3a/2)$. This enables us to express $\phi(x)$ and $g_0(x)$ in terms of the Whittaker functions,[29] similar to Ref. 22 (see also Appendix A). Using such a representation, it is easy to show that

$$\phi(0)/\phi'(0) \simeq a_B/\mathcal{L}, \quad r_s \gg 1, \tag{24}$$

which, combined with Eq. (18), yields Eq. (4). With a bit more algebra, one can match Eq. (22) with another formula in region I, leading finally to Eq. (5) with η and κ given by

$$\eta = \frac{2S_3(0)}{\sqrt{2r_s}} = 2\int_0^a \frac{dx}{a}\left[\frac{\epsilon a}{e^2}\Delta U_{\rm tot}(x)\right]^{1/2}, \tag{25}$$

$$\kappa = \frac{2^{5/4}}{\sqrt{\pi}}\, e^{\xi(0)} \sqrt{\frac{\Omega(a)}{\Omega(0)}}\left[\frac{\epsilon a^3}{e^2}\, U_{\rm tot}''(a)\right]^{3/4}. \tag{26}$$

Thus, for the $N = 3$ case we were able to reduce the original complicated three-body eigenvalue problem to routine operations of solving an *ordinary* differential equation (13a) and taking two quadratures, Eqs. (23) and (25). The resultant η and κ are listed in Table I. In comparison, the FLA[11] underestimates κ by about 50%. It gets η correctly but only for $N = 3$, see more below.

One more important comment is in order. The antisymmetry of the total fermion wavefunction imposes certain selection rules[30] for the allowed values of L [see Eq. (3)] at a given total spin S. Thus, the lowest-energy L eigenstates for the two possible spin states of the $N = 3$ system, $S = 1/2$ and $S = 3/2$, are, respectively, $|L| = 1$ and 0. Since $J \ll \hbar^2/I$ at large r_s, the ground-state of the system is the $L = 0$ spin-quartet, in agreement with prior numerical work.[13,23]

IV. CASE $N > 3$

In a system of more than three electrons, the Hamiltonian that governs the important degrees of freedom, x and $\mathbf{X} = (X_2, \ldots, X_{N-1})^\dagger$, becomes

$$H_N = -\frac{\hbar^2}{2\mu}\partial_x^2 - \frac{\hbar^2}{2}\left(\mathbf{M}^{-1/2}\partial_{\mathbf{X}}\right)^\dagger\left(\mathbf{M}^{-1/2}\partial_{\mathbf{X}}\right) + U_{\rm tot}, \tag{27}$$

where

$$M_{ij}^{-1/2} = \frac{1}{\sqrt{m}}\frac{\delta_{ij} - \left(1 - \sqrt{2/N}\right)}{N-2}. \tag{28}$$

Again, the potential energy has two minima separated by a large barrier. The single-well function $\Phi_1(x, \mathbf{X})$ can be sought in the form

$$\Phi_1 = \phi(x)\exp\left[-\frac{1}{2\hbar}\Delta\mathbf{X}^\dagger\mathbf{M}^{1/2}\mathbf{\Omega}(x)\mathbf{M}^{1/2}\Delta\mathbf{X}\right], \tag{29}$$

where $\Delta\mathbf{X} = \mathbf{X} - \mathbf{X}^*$. In the language of the quantum tunneling theory, $\mathbf{X}^*(x)$ is the instanton trajectory

and $\mathbf{\Omega}(x)$ is a matrix that controls Gaussian fluctuations around the instanton. Our goal is to compute them. The usual route is to parametrize the dependence of $\mathbf{X}^*$ on x in terms of an "imaginary-time" τ, in which case $x(\tau)$ and $\mathbf{X}^*(\tau)$ must minimize the action functional

$$S_N = \int_0^\infty \frac{d\tau}{\hbar}\left[\frac{\mu}{2}(\partial_\tau x)^2 + \frac{1}{2}(\partial_\tau \mathbf{X})^\dagger \mathbf{M}\,\partial_\tau \mathbf{X} + \Delta U_{\rm tot}\right] \tag{30}$$

subject to the boundary conditions $x(0)=0$, $x(\infty)=a$, and $\mathbf{X}(\infty)=0$. Henceforth $U_{\rm tot}$ is always meant to be evaluated on the instanton trajectory and $\Delta U_{\rm tot}$ stands for the difference of its values at a given τ and at $\tau=\infty$. Repeating the steps of the derivation for the $N=3$ case, we find that Eq. (13a) for $\mathbf{\Omega}$ is still valid once we define $\boldsymbol{\omega}$ to be a positive-definite matrix such that $\boldsymbol{\omega}^2 = \mathbf{M}^{-1/2}\mathbf{\Xi}\mathbf{M}^{-1/2}$, where $\mathbf{\Xi}$ is the matrix of the second derivatives $\Xi_{ij} = \partial_{X_i}\partial_{X_j}U_{\rm tot}$. This equation has an equivalent but more elegant form in terms of τ:

$$\partial_\tau \mathbf{\Omega} = \mathbf{\Omega}^2(\tau) - \boldsymbol{\omega}^2(\tau). \tag{31}$$

Also, for practical calculations, it is convenient to take advantage of a formula

$$\mathrm{tr}\,\left(\mathbf{M}^{-1}\mathbf{\Xi}\right) + \frac{1}{\mu}\frac{\partial^2}{\partial x^2}U_{\rm tot}(x) = \frac{1}{2\mu}\sum_{\substack{i,j=0\\ i\neq j}}^{N-1} U''(x_i - x_j)\,. \tag{32}$$

As for Eqs. (13b) and (23), they require only the replacement $\Omega \to \mathrm{tr}\,\mathbf{\Omega}$,

$$\left\{\frac{\hbar^2}{2\mu}\partial_x^2 - U_{\rm tot}(x) - \frac{\hbar}{2}\,\mathrm{tr}\,\mathbf{\Omega}(x) + E\right\}\phi(x) = 0, \tag{33}$$

while in Eq. (26) one has to replace Ω with $\det\mathbf{\Omega}$.

Finally, instead of Eq. (25) we have $\eta = 2S_N/\sqrt{2r_s}$, consistent with the notion that the main exponential dependence of J is always determined by the tunneling action.

V. CALCULATION OF THE INSTANTON

A few properties of the instanton follow from general considerations. The dimensional analysis of Eq. (30) yields $S_N \propto \sqrt{r_s}$, so that η is indeed just a constant. Also, from the symmetry of the problem, $X_{N+1-j}(\tau) = -X_j(\tau)$. Thus, in the special case of $N=3$, the instanton trajectory is trivial: $X_2 \equiv 0$, i.e., the $j=2$ electron does not move. This is why we were able to compute S_3 in a closed form, Eq. (21). For $N>3$ the situation is quite different: all electrons [except $j=(N+1)/2$ for odd N] do move. In order to investigate how important the motion of electrons distant from the $j=0,1$-pair is let us consider the $N=\infty$ (*quantum wire*) case, where the far-field effects are the largest. If X_j's were small, we could expand $\Delta U_{\rm tot}$ in Eq. (30) to the second order in X_j to obtain the harmonic action

$$S_h = \frac{1}{2}\frac{m}{\hbar}\int\frac{dk}{2\pi}\int\frac{d\omega}{2\pi}\,|u_{k\omega}|^2\left[\omega^2 + \omega_p^2(k)\right], \tag{34}$$

where $u_{k\omega}$ is the Fourier transform of $u_j(\tau) \equiv x_j - x_j^0$, electron displacement from the classical equilibrium position $x_j^0 \equiv (j-1/2)a$, $j\in\mathbb{Z}$, and

$$\omega_p(k) \simeq s_0 k \ln^{1/2}\left(\frac{4.15}{ka}\right), \quad s_0 \equiv \sqrt{\frac{e^2}{\epsilon\mu a}} \tag{35}$$

is the plasmon dispersion in the 1D WC (the logarithmic term is due to the long-range nature of the Coulomb interaction). Minimization of S_h with the specified boundary conditions yields

$$u_j(\tau) \propto \frac{v x_j^0}{(x_j^0)^2 + v^2\tau^2}, \quad v \simeq \frac{s_0}{2}\ln\frac{(x_j^0)^2 + s_0^2\tau^2}{a^2}. \tag{36}$$

Substituting this formula into Eq. (34), we find that the contributions of distant electrons to S_h rapidly decay with $|j|$. Since $u_j(\tau)$'s are small at large j and τ we expect that these j- and τ-dependencies are rendered correctly by the harmonic approximation. Thus, a fast convergence of η to its thermodynamic limit is expected as N increases.

Encouraged by this conclusion, we undertook a direct numerical minimization of S for the set of N listed in Table I using standard algorithms of a popular software package MATLAB. The optimal trajectories that we found for the case $N=8$ are shown in Fig. 3. In agreement with our earlier statement, $u_j(0)$ reach a finite fraction of a. This collective electron motion lowers the effective tunneling barrier and causes η to drop below its FLA value, although only by 0.7%, see Table I. Further decrease of η as N increases past 8 is beyond the accuracy of the employed minimization procedure.

Let us now discuss the prefactor κ. In the inset of Fig. 3 we plot $\mathrm{tr}\,\mathbf{\Omega}(x)$ computed by solving Eq. (31) numerically. To reduce the calculational burden, we set $\mathbf{X}^*(\tau)\to 0$ instead of using the true instanton trajectory. The error in κ incurred thereby is $\sim 2\%$ (see Sec. VII). In comparison, the FLA, where $\mathrm{tr}\,\mathbf{\Omega}(x) = \mathrm{const}$, yields κ about 50% smaller than the correct result, similar to $N=3$.

VI. ALTERNATIVE DERIVATION OF THE EXCHANGE CONSTANT

The relation (4) between the exchange constant J and the PCF of the spinless system — which is one of our main results — was derived in Sec. III assuming $r_s \gg 1$. In this section we show that in ultrathin wires, $\mathcal{L} \equiv \ln(a_B/R) \gg 1$, this relation holds under a more general condition: with an accuracy $O(1/\mathcal{L})$, it remains valid as long as the *strong* spin-charge separation

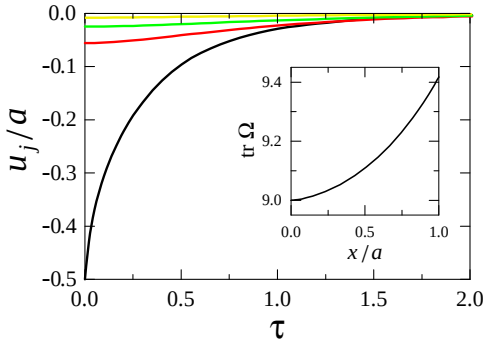


FIG. 3: (Color online) The instanton trajectories of $1 \le j \le 4$ electrons in the $N = 8$ Wigner molecule on a ring. Inset: $\mathrm{tr}\,\mathbf{\Omega}(x)$. The units of τ and $\mathbf{\Omega}$ are $\sqrt{2}a/s_0$ and its inverse.

persists, $J \ll E_F \sim \hbar^2/ma^2$. In particular, it applies at $r_s \sim 1$, i.e., in a parametric regime which has been notoriously difficult for a controlled theoretical analysis. Therefore, we think that Eq. (4) amounts to some definite progress. The fundamental reason for the broad domain of validity of Eq. (4) is that in 1D the $1/r$ fall-off of the Coulomb potential (2) constitutes a sufficiently rapid decay. In fact, the relations of type of Eq. (4) are generic for 1D models in which electrons interact via the potential $U(r) \sim 1/r^\alpha$ with $\alpha \ge 1$. Known to us physical realizations of $\alpha > 1$ cases include (i) $\alpha = 3$, which occurs when the bare Coulomb interaction is screened by a nearby metallic plane,[22] and (ii) $\alpha = 2$, where the screening is accomplished by a half-plane, see Sec. VII below.

In order to derive Eq. (4) for the unscreened Coulomb interaction ($\alpha = 1$) we make a connection with a previous work of one of us[22] where it was shown that in ultrathin wires an unusual correlated regime — Coulomb Tonks gas (CTG) — exists in the window $1/\mathcal{L} \ll r_s \ll 1$. In the CTG, unlike in a WC, the long-range tails of the Coulomb potential have no important effect on the spin degree of freedom. To the leading order in r_s, the Coulomb interaction (2) acts simply as a strong short-range repulsion. This allows one to characterize its effect solely in terms of the transmission coefficient $t(q)$ for a two-electron collision with the relative momentum q. Based on this observation, the following formula for J was derived[22]

$$J = \frac{\hbar^2}{m}\int \frac{dq}{2\pi}\tilde{g}_0(q)q\,\mathrm{Im}\,t(q), \quad J \ll E_F. \tag{37}$$

To see how it leads to Eq. (4) we first note that for the potential (2) the transmission coefficient has the form[22]

$$t(q) = \frac{iq}{iq - (m/\hbar^2)c(q)}, \quad q \gg \frac{1}{a_B}, \tag{38}$$

where $c(q) = 2(e^2/\epsilon)\ln(1/2qR)$. The slow (in this case, logarithmic) dependence of c on q is crucial here and it is precisely due to the aforementioned fast decay of $U(r)$ with distance. As explained in Ref. 22, in the CTG regime the integral in Eq. (37) is dominated by $q \sim 1/a$; therefore, to the order $O(1/\mathcal{L})$ one can replace $c(q)$ by $c(1/a)$ and then by $2(e^2/\epsilon)\mathcal{L}$. Finally, it is permissible to neglect iq in the denominator of Eq. (38), thereupon Eq. (37) becomes identical to Eq. (4).

Our next task is to show that Eq. (4) holds not only in the two limiting case (CTG and WC) but also everywhere in between. We do so with the help of a formalism that can be considered a continuum analog of the Schrieffer-Wolfe transformation in the Hubbard model, in particular, in its 1D version.[31]

Let $j \in \mathbb{Z}$ label electrons in the order of increasing instantaneous coordinates x_j. Then, by construction, the coupling constant J refers to the exchanges of nearest-neighbors, say, $j = 0$ and $j = 1$. This coupling is suppressed because in order to exchange, the two electrons have to approach each other very closely and at that moment their mutual Coulomb repulsion $U(x)$ is very strong. Let a_c be a suitable short-range cutoff. Since we are interested in the physics at the energy scale J, it should be possible in principle to "integrate out" the processes at the much higher energy scale $U(a_c)$. In doing so one would trade the bare Hamiltonian H for a renormalized one, $H + H_\sigma$, which however yields the same value of the effective coupling J. Traditionally, this renormalization program is accomplished by incrementally increasing a_c from zero to a, the natural upper limit. In particular, the Hamiltonian (3) can be viewed as the final result of such a renormalization. However, it is fully legitimate to stop the process while a_c is still much smaller than a. At this stage the charge correlations at scales shorter than a_c can not longer be studied because the corresponding degrees of freedom are already integrated out. This implies that the form of H_σ is not unique: H_σ may differ in their structure on scales $x < a_c$ as long as the resultant J is unchanged. Therefore, it should be possible to choose H_σ in the form

$$H_\sigma = U_\sigma(x)(\mathbf{S}_0\mathbf{S}_1 - 1/4) + \Delta c\,\delta(x). \tag{39}$$

It is especially convenient to take the limit $\Delta c \to \infty$, in which electrons behave as impenetrable particles. Although thus renormalized Hamiltonian forbids the pair-exchange in the real space, if the choose $U_\sigma(x)$ correctly, the spin exchange rate J, which is the only observable manifestation of an interchange of identical particles, would be preserved. A familiar example of such a H_σ on a lattice is the added term

$$\frac{4t^2}{U}\left(\mathbf{S}_i\mathbf{S}_{i+1} - \frac{1}{4}n_i n_{i+1}\right) \tag{40}$$

complemented with the no-double-occupancy constraint (i.e., $U \to U + \Delta U = \infty$) in the theory of a large-U 1D Hubbard model.[31]

The choice of $U_\sigma(x)$ in Eq. (39) is again not unique. To readily get the result we want, we require that (i) $U_\sigma(x)$ decays exponentially with x and (ii) its effect on any wavefunction $\Phi(x)$ that vanishes at $x = 0$ is adequately

described by the first-order perturbation theory. Under such conditions the spin dynamics is captured correctly to the leading order in $1/\mathcal{L}$ as long as $U_\sigma(x)$ satisfies the constraint

$$I_2 \equiv \int_0^\infty dx\, x^2 U_\sigma(x) = \frac{\hbar^2}{m}\frac{a_B}{\mathcal{L}}. \tag{41}$$

The proof is relegated to Appendix A. From this point the derivation of Eq. (4) is straightforward. After the renormalization, the infinitely strong δ-function included in H_σ causes the orbital wavefunction of the system to vanish at $x = 0$, so that the perturbation theory in U_σ now applies. To the leading order we can compute the sought exchange constant J by averaging U_σ over such a wavefunction or equivalently over the renormalized PCF $g_{\rm ren}(x)$:

$$J = \frac{1}{2}\int_{-\infty}^{\infty} U_\sigma(x) g_{\rm ren}(x) dx. \tag{42}$$

(The factor 1/2 accounts for the two-body nature of the interaction.) Let us discuss $g_{\rm ren}(x)$ in more detail. First of all, under the conditions of a strong spin-charge separation the PCF a spinful (g) and spinless (g_0) systems are always very similar. Before the renormalization (for the original Hamiltonian) both functions are peaked at $x \sim a$ and rapidly decrease as $x \to 0$, albeit only $g_0(x)$ vanishes at $x = 0$, while $g(0)$ is simply very small. Once H_σ is added, $g(x)$ gets replaced by the function $g_{\rm ren}(x)$, which vanishes at $x = 0$ and thus is nearly identical to the original g_0 at *all* x. The PCF $g_0(x)$ of the spinless system does not change appreciably. Since $U_\sigma(x)$ is short-range, the integral in Eq. (42) is dominated by small x. Therefore, we can substitute the expansion $g_{\rm ren}(x) \simeq g_0(x) \simeq g_0''(0)x^2/2$ in place of the full $g_{\rm ren}(x)$. Comparing the result with Eq. (41), we arrive at Eq. (4).

This alternative route to the derivation of Eq. (4) has the advantage of being valid in a broader range of r_s compared to Herring's method[26] originally designed for the quasiclassical case $r_s \gg 1$. It may also be more intuitive because the Hubbard-model expression (40) is widely known. Finally, it can be easily generalized to other interaction types, as discussed in the next section.

VII. AN INTEGRABLE MODEL WITH A SCREENED COULOMB INTERACTION

Our instanton calculation in Sec. IV is expected to be asymptotically exact in the limit of large r_s. However it is a good practice to verify whenever possible that any given calculation is free of inadvertent arithmetic or coding mistakes. With this in mind we applied our method also to the interaction law

$$U(r) = \frac{\hbar^2}{m}\frac{\lambda(\lambda-1)}{(r+R)^2}, \tag{43}$$

which is similar to the celebrated Calogero-Sutherland-Moser (CSM) model,[32] except for the short-range cutoff R in $U(r)$. Without this cutoff (i.e., for $R = 0$) the potential U is impenetrable, so that $J = 0$. With a finite cutoff a weak tunneling through the potential barrier $U(r)$ is possible, which imparts the system with a spin dynamics and has interesting experimental implications (see Appendix B). But to finish with the theoretical part, let us first focus on the original CSM model, $R = 0$. This is a good test case because, on the one hand, a number of exact analytical results are available here. On the other hand, the model also possesses a WC regime, at $\lambda \gg 1$, so that the corresponding PCF $g_0(x)$ should be calculable by our method. According to the exact results,[32,33] the PCF behaves as

$$g_0(x) \simeq \frac{\varkappa\sqrt{\lambda}}{a}\left(C\frac{x}{a}\right)^{2\lambda}, \quad x \to 0. \tag{44}$$

For the three-electron molecule on a ring the coefficients C and $\varkappa$ can be computed in a straightforward manner directly from the exact[32] three-body wavefunction:

$$N = 3,\ \lambda \gg 1: \quad C = \frac{8\pi}{9\sqrt{3}}, \quad \varkappa = \sqrt{\frac{8\pi}{27}}. \tag{45}$$

For $N = \infty$ the derivation is much more involved, but the result[33,34] is also known:

$$\frac{C}{2\pi\lambda} = \left[\frac{\Gamma^3(\lambda+1)\sqrt{3/\pi\lambda}}{\Gamma(2\lambda+1)\Gamma(3\lambda+1)}\right]^{1/(2\lambda)}, \quad \varkappa = \sqrt{\frac{\pi}{3}}, \tag{46}$$

where $\Gamma(z)$ is Euler gamma-function.[29] In the WC limit the first formula reduces to

$$C = \frac{e\pi}{3\sqrt{3}}, \quad \lambda \gg 1. \tag{47}$$

The calculation of $g_0(x)$ by the instanton method is virtually the same as in Sec. V except for two minor changes. First, the quasiclassical approximation is valid down to $x = 0$, i.e., there is no region I in Fig. 2. Second, to handle the logarithmic divergence of the tunneling action, inherent to the CSM model, one has to impose a different boundary condition for the instanton, $x(\tau = 0) = z$, which makes S_N a function of z [similar to S_3 being a function of x in Eq. (21)]. At small z it behaves as

$$S_N \simeq \sqrt{\lambda(\lambda-1)}\,[\ln(a/z) - \Delta S]. \tag{48}$$

Replacing $\sqrt{\lambda(\lambda-1)}$ by $\lambda - 1/2$, we find [cf. Eqs. (25) and (26)]

$$C = e^{\Delta S}, \quad \varkappa = \frac{e^{\xi(0)-\Delta S}}{\sqrt{\pi}\left(l\sqrt{\lambda}/a\right)^3}\sqrt{\frac{\det \mathbf{\Omega}(a)}{\det \mathbf{\Omega}(0)}} \tag{49}$$

(it is easy to see that $\varkappa$ is a λ-independent constant).

Remarkably, for $N = 3$ the solution of Eq. (13a) and all the necessary quadratures can be done analytically. Using the expression for total potential energy

$$U_{\rm tot}\,(x) = \frac{\pi^2}{9}\frac{\hbar^2}{m}\frac{\lambda(\lambda-1)}{a^2} \times \left[\frac{1}{\sin^2(\pi x/3a)} + \frac{2}{\cos^2(\pi x/6a)} - 4\right], \quad (50)$$

we derive (for $\lambda \gg 1$)

$$\phi\,(x) = \left[4\sin\left(\frac{\pi x}{3a}\right)\left(1+\cos\frac{\pi x}{3a}\right)\right]^{\lambda}, \qquad \Omega\,(x) = \frac{\pi^2}{3}\frac{\hbar}{ma^2}\frac{\lambda}{\cos^2(\pi x/6a)}, \quad (51)$$

which allows one to recover the exact result Eq. (45).

To check if we can also reproduce Eq. (47) for $N = \infty$, we calculated ΔS and $\varkappa$ numerically for $4 \le N \le 10$ and fitted them to cubic polynomials in $1/N$. Extrapolating the fits to $N = \infty$, we obtained $\exp(\Delta S) = 1.6438(4)$ and $\varkappa = 1.04$ compared to the exact values 1.6434 and 1.02, respectively. We attribute the 2% discrepancy in $\varkappa$ to our choice not to use the true instanton trajectory in Eq. (31). Apparently, our method has successfully passed this test; thus, our results for the unscreened Coulomb interaction (Table I) should also be reliable.

Let us now consider the case with a small but nonzero cutoff, $0 < R \ll a$. As explained in Appendix B, this model can be relevant for the existing experimental setup of Auslaender *et al.*[15] provided the electron density can be made low enough. Therefore, the calculation of J has an independent significance. This calculation is again similar to that for the case of the bare Coulomb interaction, Sec. VI, except that instead of Eq. (41) the constraint on the effective potential becomes

$$I_{2\lambda} \equiv \int_0^\infty dx\, x^{2\lambda} U_\sigma\,(x) = \frac{\pi}{\lambda-1}\frac{\hbar^2}{m}R^{2\lambda-1}. \quad (52)$$

(For derivation, see Appendix A.) Consequently, Eq. (4) is replaced with

$$J = I_{2\lambda}a_c^{-2\lambda}g_0(a_c), \quad R \ll a_c \ll a. \quad (53)$$

Since R is parametrically smaller than a, it is permissible to substitute Eqs. (44) and (46) into the last formula, which yields

$$J = \gamma\frac{\hbar^2}{ma^2}\left(\frac{R}{a}\right)^{2\lambda-1}, \quad (54)$$

$$\gamma = \frac{1}{2\lambda(\lambda-1)}\frac{(2\pi\lambda)^{2\lambda+1}\Gamma^3(\lambda+1)}{\Gamma(2\lambda+1)\Gamma(3\lambda+1)}. \quad (55)$$

From Eq. (54) one concludes that the strong spin-charge separation in the model in hand may arise for an arbitrary $\lambda > 1$ provided $R/a \ll \min\{1, \lambda-1\}$. In the experimental setup of Auslaender *et al.*[15], where this model can be realized physically, we estimate $R \approx 0.7a_B$ and $\lambda = 1.5$–2, see Appendix B, so that $\gamma = 36$–40. Our formula predicts that as the electron density is reduced, a fairly rapid *algebraic* fall-off Eq. (54) of J should become observable, provided the disorder effects do not intervene. The crossover from high to low-density behavior is discussed in more detail in the next section where we give arguments that the strong spin-charge separation sets in already at rather modest r_s.

VIII. VALIDITY DOMAIN OF THE OBTAINED FORMULAS AND NUMERICAL ESTIMATES

A. Intermediate densities

Returning to the case of the unscreened Coulomb interaction, an important practical question is the relevance of the obtained formulas for a more common experimental situation of $r_s \sim 1$. Although Eq. (4) reduces this question to an easier problem of calculating the PCF of spinless fermions, at such r_s it still has to be done numerically. Deferring this effort for a possible future work, we attempted to see whether one can estimate J at $r_s \sim 1$ by a simple interpolation between the high-density limit $r_s \ll 1$, corresponding to the CTG,[22] and the low-density WC limit, $r_s \gg 1$, studied in this work.

Using Eq. (37) with $\tilde{g}_0(q)$ computed to the linear order in r_s (per Ref. 22) we obtained for the CTG

$$J = \frac{e^2}{\epsilon a_B}\frac{\pi^2}{24 r_s^3 \mathcal{L}}\left[1 - \frac{2(3+\pi^2)}{3\pi^2}r_s\right] + O\left(\frac{1}{\mathcal{L}^2}\right), \quad (56)$$

which is valid for $1/\mathcal{L} \ll r_s \ll 1$. We plotted this dependence in Fig. 4 together with the prediction of Eq. (5) for the infinite-wire WC. As one can see, a smooth interpolation between the two is entirely possible. In fact, the curves match almost seamlessly around $r_s \sim 0.9$ where a tiny gap has been left on purpose to separate them from each other. However, we must warn the reader that at such r_s the high-density approximation of Eq. (56) certainly needs higher-order corrections (taken literally, it would give negative J at $r_s > 1.15$). Similarly, Eq. (5) is likely to have its own non-negligible corrections at such r_s. Thus, one should regard Fig. 4 as the indication that the crossover from the CTG to the WC occurs at $r_s = 1$–2. To put it another way, we expect that our Eq. (5) becomes quantitatively accurate at $r_s \gtrsim 2$. This conclusion seems to be in agreement with the numerical result of Ref. 8 that the 1D WC is well-formed already at $r_s > 4$. To get an idea of the size of J, we can use parameters $r_s = 4$, $a_B = 1.5$ nm, and $\epsilon = 1$, which are relevant for the experiment of Jarillo-Herrero *et al.*[10] For this set of numbers Eq. (5) yields

$$J \approx 1 \text{ K}. \quad (57)$$

Unfortunately, the lowest temperature in that experiment was 0.3 K, so the exchange correlations may have been strongly affected. We leave the investigation of the

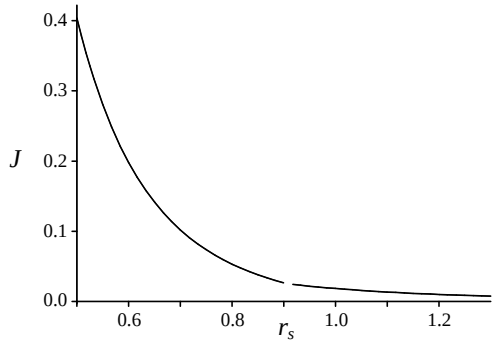


FIG. 4: Exchange constant in units of $e^2/\epsilon a_B$ as a function of r_s for $a_B/R = 100$. The left curve is computed according to Eq. (56), the right one is per Eq. (5).

finite-temperature effects for a future study. We also hope that lower temperatures can be achieved in the next round of experiments, so that we would be in a better position to check our predictions.

B. Thicker wires

Another question that we wish to briefly address is the behavior of the exchange constant in a wire of radius $R \gtrsim a_B$. This parametric regime is more common than that of ultrathin wires, $R \ll a_B$, and so it needs to be investigated.

In regards to the WC limit, the correction to parameter η of Eq. (5) due to a finite R has been studied by Klironomos *et al.*[21] These authors pointed out that in the wires with radius $R \gtrsim a_B$ the problem of spin exchange cannot be treated as a purely 1D one from the outset. They found that the tunneling trajectories of the primary electron pair avoid the head-on collision by deviating off the wire center in the transverse direction by a certain amount r_0 each. For the parabolic confinement potential $U_{\rm con}(r_\perp) = (\hbar^2/2mR^2)(r_\perp/R)^2$ it is easy to find the estimate $r_0 \sim (R^4/a_B)^{1/3}$ by balancing the Coulomb repulsion and the lateral confinement forces at the point of the closest approach. As long as $r_0 \ll a$, it remains possible to modify the interaction potential $U(x)$ to take this effect into account. [At the simplest level, it is sufficient to replace R by $2r_0$ in Eq. (2).] Thereafter, one can still treat the problem as 1D.[39]

In thick wires the relationship between the PCF and the exchange constant would differ from Eq. (4). Of primary importance here is the small-distance behavior of $U(x)$. When $r_0 \gg a_B$, the interaction potential becomes so smooth near $x = 0$ that it can be approximated by a constant $U(0) \sim e^2/2\epsilon r_0$. Following the method outlined in Appendix A, one arrives at the relation

$$J = \frac{e^2 a_B}{2\epsilon} a_0 g_0''(x), \quad a_0 = \frac{\hbar}{\sqrt{mU(0)}} \sim (R^2 a_B)^{1/3}. \quad (58)$$

We see that the factor $\mathcal{L}$ in Eq. (4) gets replaced with $a_B/a_0 \ll 1$.[40]

In the case of intermediate-width wires, $R \sim a_B$, one can use $a_0 = a_B$ for order-of-magnitude estimates; however, the exact value of the coefficient a_0 and therefore κ in Eq. (5) would depend on the details of the confinement potential $U_{\rm con}(\mathbf{r}_\perp)$.

IX. CONCLUSIONS

In this paper we have developed a method for a controlled calculation of the exchange constant J in correlated 1D electron systems to the leading order in the large parameter r_s. This method is able to reproduce a number of exact results for integrable models, which is a strong indicator of its validity. In comparison to a prior uncontrolled calculation[11] of the same quantity for the Coulomb case, our method brings a small correction of about 0.7% to the coefficient in the exponential term; however, the correction to the pre-exponential factor is large, about 50%.

Our another main result — the relation between J and the pair-correlation function of spinless electrons — is a promising ground for an attack on the regime of intermediate concentrations, $r_s \sim 1$, which has so far been difficult for a controlled analytical study. We demonstrated that a very smooth interpolation between the high and low-density asymptotic is possible based already on the results in hand (Fig. 4).

Finally, we have applied our method to a number of realistic interaction potentials corresponding to different geometries of experimental setup. Apart from nearly impenetrable Coulomb interaction in ultrathin quantum wires and quantum rings, which has been the primary focus of this work, we have studied penetrable smooth interactions that take place in the wires of intermediate width and a screened $1/x^2$ interaction that is realized, e.g., when the wire is located near a metallic half-plane.

These findings have direct implications for the energy spectroscopy of spin-splitting in nanoscale quantum rings[4,5,6] and 1D quantum dots.[9,10,15] Some estimates were given in Secs. VII and VIII above. They should be especially accurate in the ultrathin-wire limit[22] $\mathcal{L} = \ln(a_B/R) \gg 1$ that can be achieved in carbon-nanotube field-effect transistors with high-k dielectrics.[35]

In long 1D wires, the exchange coupling J determines the velocity of the elementary spin excitations

$$v_\sigma = \frac{\pi}{2}\frac{Ja}{\hbar}, \quad (59)$$

which can nowadays be measured by tunneling,[15] angle-resolved photoemission,[16] or deduced from the enhancement of the spin susceptibility and electron specific heat.[22] Our result for v_σ reads (cf. Table I)

$$v_\sigma/v_F = 17.8\, r_s^{3/4} e^{-\eta\sqrt{2r_s}}/\mathcal{L}, \quad \eta = 2.7978(2), \quad (60)$$

where $v_F = (\pi/2)(\hbar/ma)$ is the Fermi velocity.

Acknowledgments

The support from the A. P. Sloan Foundation and C. & W. Hellman Fund is gratefully acknowledged. We thank A. D. Klironomos, R. R. Ramazashvili, and K. A. Matveev for discussions.

APPENDIX A: SPIN-DEPENDENT PART OF THE EFFECTIVE POTENTIAL

In this Appendix we derive Eqs. (41), (52), and (58). Let $x \equiv x_1 - x_0$ be the relative distance between the two electrons for which we want to compute the exchange coupling. Consider the orbital part of the many-body wavefunction Φ,which is a function of x and $N-1$ other coordinates. In principle, Φ is different for different many-body spin states. Nonetheless, under the condition $J \ll E_F$ where only nearest-neighbor exchanges are important, at small x function Φ depends primarily on the total spin of the given pair. The triplet-state wavefunction $\Phi_t(x)$ is odd and therefore $\Phi_t(0) = 0$. In the singlet state we have $\Phi_s(x)$ which is even and finite at $x = 0$ (cf. Sec. III). However, because of the strong Coulomb repulsion $\Phi_s(0)$ is very small. At $x \ll a$ the two electrons of interest are under a large Coulomb barrier and it is legitimate to assume that Φ_t and Φ_s are functions of only x, the fastest variable in the problem. Our goal is to choose $U_\sigma(x)$ that reproduces the difference between Φ_s and Φ_t at the level of the first-order perturbation theory. This is achieved if there exists a window $a_c \ll x \ll a$, where the following equation is satisfied:

$$\Phi_t(x) - \Phi_s(x) = \int_0^\infty dx' G(x,x') U_\sigma(x') \Phi_t(x'). \qquad \text{(A1)}$$

Here the Green's function G is the solution of

$$\left[-\frac{\hbar^2}{2\mu}\partial_x^2 + U(x) - E \right] G(x,x') = -\delta(x-x'), \qquad \text{(A2)}$$

where $E \sim e^2/\epsilon a$ is the total energy. At the end of the calculation one can verify that the final result [Eq. (41)] holds independently of the precise value of E up to terms $O(1/\mathcal{L})$.

Our next step is to use the usual representation of G,

$$G(x,x') = -\frac{2\mu}{\hbar^2 Q} \begin{cases} u(x)v(x'), & x > x', \\ v(x)u(x'), & x < x', \end{cases} \qquad \text{(A3)}$$

in terms of two linearly-independent solutions of the (homogeneous) Schrödinger equation (A2). The solution $u(x)$ initially decays exponentially with x and then turns into a wave propagating towards $x = +\infty$. The other solution, $v(x)$ has a node at $x = 0$, exhibits an exponential rise and finally becomes a standing wave. The quantity $Q = uv' - u'v$ is their Wronskian.

Wavefunctions Φ_s and Φ_t are the linear combinations of u and v that are even and odd in x, respectively. For x at which Eq. (A1) is valid, $\Phi_t \simeq \Phi_s \simeq \text{const} \times v(x)$. Using this property and some trivial algebra, we get

$$\int_0^\infty dx U_\sigma(x) v^2(x) = \frac{\hbar^2}{2\mu} \frac{Q^2}{u(+0)u'(+0)}. \qquad \text{(A4)}$$

For the Coulomb case [Eq. (2)] u and v can be expressed in terms of Whittaker functions[29] $W_\alpha(z)$ and $M_\alpha(z)$ (see an earlier remark in Sec. III and Ref. 22):

$$\begin{aligned} u(x) &= W_{-i\nu,1/2}[i(x-R)/b], \\ v(x) &= M_{-i\nu,1/2}[i(x-R)/b] \\ &\quad - M_{-i\nu,1/2}(-iR/b)u(x)/u(0), \end{aligned} \qquad \text{(A5)}$$

where $b = \hbar/(8\mu E)^{1/2}$ and $\nu = b/a_B \sim \sqrt{r_s} \gg 1$. Using the relations[29] $W_{-i\nu,1/2}(0) = 1/\Gamma(1+i\nu)$ and $M_{-i\nu,1/2}(iz) \simeq iz$ at $z \ll 1$, we find $Q = i/\Gamma(1-i\nu)b$. Substituting these results into Eq. (A4) and dropping terms that are small in the parameter $R/a_B \ll 1$, we recover Eq. (41).

Similarly, for the CSM model [Eq. (43)] u and v are given by

$$\begin{aligned} u(x) &= \sqrt{x} H^{(1)}_{\lambda-1/2}(qx), \\ v(x) &= \sqrt{x} J_{\lambda-1/2}(qx), \end{aligned} \qquad \text{(A6)}$$

where $q = \sqrt{mE}/\hbar$, and $H^{(1)}_\nu$, J_ν are the Hankel and the Bessel functions of the first kind,[29] respectively. Their Wronskian is given by $W\{u,v\} = 1/i\pi(\lambda - 1/2)$, and their known asymptotic behavior leads in this case to the formulas

$$\begin{aligned} u(R) &\simeq \Gamma(\lambda - 1/2) R^{1-\lambda}/i\pi, \\ u'(R) &\simeq (1-\lambda)u(R)/R, \\ v(R) &\simeq R^\lambda/\Gamma(\lambda + 1/2), \end{aligned} \qquad \text{(A7)}$$

so that the constraint on $U_\sigma(x)$ is expressed by Eq. (52).

Finally, in thick 1D wires, where $U(x) \simeq \text{const}$ at small x (Sec. VIII), the solutions of Eq. (A2) are $u(x) = \exp(-x/a_0)$ and $v(x) = \sinh(x/a_0)$, where $a_0 = \hbar/\sqrt{mU(0)}$. These formulas leads to Eq. (58).

APPENDIX B: PHYSICAL REALIZATION OF THE CALOGERO-SUTHERLAND-MOSER MODEL

The CSM interaction law can be realized experimentally if the 1D wire is positioned nearby a metallic half-plane, parallel to its edge, see Fig. 5. In this configuration the interaction potential has the Coulomb form [Eq. (2)] only at small x. Below we show that at larger distances, $|x| \gg D$, the interaction changes to the CSM law $U(x) \simeq A/x^2$, due to the screening effect of the

metal. For simplicity, let us assume that the metallic half-plane is an ideal conductor and that $x \gg R$. In this case $U(x) = V(x, D, \theta)$, where V is the solution of the following electrostatic problem:

$$\nabla^2 V(\mathbf{r}) = \left(\frac{\partial^2}{\partial x^2} + \frac{1}{\rho}\frac{\partial}{\partial \rho}\rho\frac{\partial}{\partial \rho} + \frac{1}{\rho^2}\frac{\partial^2}{\partial \varphi^2} \right) V(x, \rho, \varphi)$$
$$= -\frac{4\pi e^2}{\epsilon D}\delta(x)\delta(\rho - D)\delta(\varphi - \theta), \qquad \text{(B1)}$$
$$V(\mathbf{r}) = 0, \quad \varphi = \pm\pi. \qquad \text{(B2)}$$

Using standard methods (cf. Ref. 36 and references therein) one can express V in terms of elliptic integrals. However, for a general θ, such expressions are not very illuminating. An exception is the case $\theta = 0$, where V takes the form

$$V(\mathbf{r}) = \frac{2}{\pi\epsilon}\frac{e^2}{|\mathbf{r} - \mathbf{D}|}\arctan\frac{\sqrt{2D\rho\,(1 + \cos\varphi)}}{|\mathbf{r} - \mathbf{D}|}, \qquad \text{(B3)}$$

where $\mathbf{D} = (0, 0, D)$. This formula can be verified by the direct substitution into Eqs. (B1) and (B2). For the intra-wire interaction law we obtain

$$U(x) = \frac{2}{\pi\epsilon}\frac{e^2}{|x|}\arctan\frac{2D}{|x|}, \qquad \text{(B4)}$$

so that $A = 4De^2/\pi\epsilon$ in this case. We can also show that for an arbitrary $-\pi < \theta < \pi$ the coefficient A is given by

$$A = \frac{2D}{\pi}\frac{e^2}{\epsilon}\,(1 + \cos\theta)\,. \qquad \text{(B5)}$$

First we note that the Fourier transform of U must have the form $\tilde{U}(q) \simeq \tilde{U}(0) - \pi A|q|$ at small q. On the other hand, $\tilde{U}$ is given by the generalized Fourier series

$$\tilde{U}(q) = \frac{2e^2}{\epsilon}\sum_{n=1}^{\infty}\left[1 - (-1)^n\cos n\theta\right] I_{n/2}(qD)K_{n/2}(qD),$$

where I_ν and K_ν are the modified Bessel functions of the first and the second kind, respectively.[29] The non-analytic $|q|$-contribution comes only from the $n = 1$ term in the series. Using the formulas[29] $I_{1/2}(z) = (2/\pi z)^{1/2}\sinh z$ and $K_{1/2}(z) = (\pi/2z)^{1/2}\exp(-z)$, we arrive at Eq. (B5).

The geometry of Fig. 5(b) has been realized in the experiment of Auslaender *et al.*[15], where the role of the metallic half-plane was played by a two-dimensional electron gas. In contrast to our idealized electrostatic model, the two-dimensional metal has a non-zero Thomas-Fermi screening radius $r_{\rm TF}$. We expect that in this situation the only change in Eq. (B5) is the replacement of D by $D + r_{\rm TF}$. This yields the following estimate for the parameter λ in Eq. (43):

$$\lambda = \frac{1}{2} + \sqrt{\frac{1}{4} + \frac{2}{\pi}\frac{D + r_{\rm TF}}{a_B}(1 + \cos\theta)}. \qquad \text{(B6)}$$

In the experimental setup of Ref. 15 $D \sim a_B \sim r_{\rm TF}$, so that $\lambda = 1.5$–2.

[1] R. Saito, G. Dresselhaus, and M. S. Dresselhaus, *Physical Properties of Carbon Nanotubes* (Imperial College Press, London, 1998).
[2] Y. Huang, X. Duan, Y. Cui, L. J. Lauhon, K.-H. Kim, and C. M. Lieber, Science **294**, 1313 (2001).
[3] A. Nitzan and M. A. Ratner, Science **300**, 1384 (2003).
[4] A. Lorke, R. J. Luyken, A. O. Govorov, J. P. Kotthaus, J. M. Garcia, and P. M. Petroff, Phys. Rev. Lett. **84**, 2223 (2000); R. J. Warburton, C. Schäflein, D. Haft, F. Bickel, A. Lorke, K. Karrai, J. M. Garcia, W. Schoenfeld, and P. M. Petroff, Nature (London) **405**, 926 (2000).
[5] A. Fuhrer, T. Ihn, K. Ensslin, W. Wegscheider, and M. Bichler, Phys. Rev. Lett. **93**, 176803 (2004).
[6] M. Bayer, M. Korkusinski, P. Hawrylak, T. Gutbrod, M. Michel, and A. Forchel, Phys. Rev. Lett. **90**, 186801 (2003).
[7] H. J. Schulz, Phys. Rev. Lett. **71**, 1864 (1993).
[8] R. Egger, W. Häusler, C. H. Mak, and H. Grabert, Phys. Rev. Lett. **82**, 3320 (1999).
[9] S. B. Field, M. A. Kastner, U. Meirav, J. H. F. Scott-Thomas, D. A. Antoniadis, H I. Smith, and S. J. Wind, Phys. Rev. B **42**, 3523 (1990).
[10] P. Jarillo-Herrero, S. Sapmaz, C. Dekker, L. P. Kouwenhoven, and H. S. J. van der Zant, Nature (London) **429**, 389 (2004).
[11] K. A. Matveev, Phys. Rev. B **70**, 245319 (2004).
[12] C. Herring, Rev. Mod. Phys. **34**, 631 (1962);
[13] S. M. Reimann and M. Manninen, Rev. Mod. Phys. **74**, 1283 (2002); S. Viefers, P. Koskinen, P. Singha Deo, and M. Manninen, Physica E **21**, 1 (2004).
[14] W. Häusler, Z. Phys. B **99**, 551 (1996).
[15] O. M. Auslaender, H. Steinberg, A. Yacoby, Y. Tserkovnyak, B. I. Halperin, K. W. Baldwin, L. N. Pfeiffer, and K. W. West, Science **308**, 88 (2005), and references therein.
[16] R. Claessen, M. Sing, U. Schwingenschlögl, P. Blaha, M. Dressel, and C. S. Jacobsen, Phys. Rev. Lett. **88**, 096402 (2002).
[17] V. V. Cheianov and M. B. Zvonarev, Phys. Rev. Lett. **92**, 176401 (2004).
[18] G. A. Fiete and L. Balents, Phys. Rev. Lett. **93**, 226401 (2004).
[19] G. A. Fiete, J. Qian, Ya. Tserkovnyak, and B. I. Halperin, Phys. Rev. B **72**, 045315 (2005).
[20] M. Fogler and E. Pivovarov, cond-mat/0504502.
[21] A. D. Klironomos, R. R. Ramazashvili, and K. A. Matveev, cond-mat/0504118.
[22] M. M. Fogler, Phys. Rev. B **71**, 161304(R) (2005).

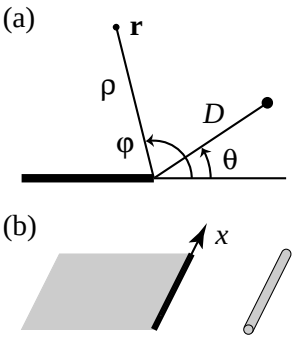


FIG. 5: The geometry of the electrostatic problem that gives rise to the CSM interaction law. (a) The cross-sectional view in a plane normal to the x-axis. The thick line symbolizes the metal half-plane, the large dot stands for the 1D wire. The drawing also indicates how the polar coordinates ρ, φ of an arbitrary point $\mathbf{r}$ are defined. (b) A three-dimensional view of the system.

[23] J. Usukura, Y. Saiga, and D. S. Hirashima, J. Phys. Soc. Jpn. **74**, 1231 (2005), and references therein.

[24] W. I. Friesen and B. Bergerson, J. Phys. C **13**, 6627 (1980).

[25] B. Szafran, F. M. Peeters, S. Bednarek, T. Chwiej, and J. Adamowski, Phys. Rev. B **70**, 035401 (2004).

[26] C. Herring, Phys. Rev. **134**, A362 (1964).

[27] L. D. Landau and E. M. Lifshitz, *Quantum Mechanics* (Pergamon, Oxford, 1977), Sec. 81.

[28] M. Roger, J. H. Hetherington, and J. M. Delrieu, Rev. Mod. Phys. **55**, 1 (1983).

[29] I. S. Gradshteyn and I. M. Ryzhik, *Table of Integrals, Series, and Products*, 6th ed., edited by A. Jeffrey and D. Zwillinger (Academic, San Diego, 2000).

[30] P. A. Maksym, Phys. Rev. B **53**, 10871 (1996); P. Koskinen, M. Koskinen, and M. Manninen, Eur. Phys. J. B **28**, 483 (2002).

[31] M. Ogata and H. Shiba, Phys. Rev. B **41**, 2326 (1990).

[32] B. Sutherland, Phys. Rev. A **4**, 2019 (1971); Int. J. Mod. Phys. B **11**, 355 (1997).

[33] P. J. Forrester, Nucl. Phys. B **388**, 671 (1992).

[34] Z. N. C. Ha, Phys. Rev. Lett. **73**, 1574 (1994).

[35] A. Javey, H. Kim, M. Brink, Q. Wang, A. Ural, J. Guo, P. Mcintyre, P. Mceuen, M. Lundstrom, and H. Dai, Nature Materials **1**, 241 (2002); B. M. Kim, T. Brintlinger, E. Cobas, M. S. Fuhrer, H. Zheng, Z. Yu, R. Droopad, J. Ramdani, and K. Eisenbeiser, Appl. Phys. Lett. **84**, 1946 (2004).

[36] M. M. Fogler, Phys. Rev. B **69**, 245321 (2004); **70**, 129902(E) (2004).

[37] G. Piacente, I. V. Schweigert, J. J. Betouras, and F. M. Peeters, Phys. Rev. B **69**, 045324 (2004).

[38] A. D. Klironomos, J. S. Meyer, and K. A. Matveev, cond-mat/0507387.

[39] Significant changes in the calculation would be required only in very thick wires with radius $R > 11\,a_B$.[21] However, in such wires the 1D WC limit can be achieved only at $r_s \gtrsim 20$ where the exchange coupling J would be unmeasurably small, see Eq. (5). At smaller r_s, other physics is likely to come into play, e.g., the 1D WC may undergo a transition into a multi-row WC[37,38] or into a liquid with multiple subband occupation.

[40] It is interesting that in the opposite limit of a short-range $U(x)$, e.g., $U(x) = c\delta(x)$, the relation between J and g_0 is formally similar, with $a_0 = 2\hbar^2/mc$, see Eqs. (37) and (38).